



Contents lists available at ScienceDirect

Materials Science in Semiconductor Processing

journal homepage: www.elsevier.com/locate/mssp

Effects of thermal annealing on the morphology of the $\text{Al}_x\text{Ga}_{(1-x)}\text{N}$ films

S. Çörekçi^{a,*}, Z. Tekeli^a, M. Çakmak^a, S. Özçelik^a, Y. Dinç^b, O. Zeybek^b, E. Özbay^c

^a Physics Department, Faculty of Art and Science, Gazi University, 06500 Ankara, Turkey

^b Department of Physics, Balikesir University, 10145 Balikesir, Turkey

^c Nanotechnology Research Center, Bilkent University, 06800 Ankara, Turkey

ARTICLE INFO

Available online 8 January 2010

Keywords:

Morphology of films

Atomic force microscope

ABSTRACT

Effects of thermal annealing on the morphology of the $\text{Al}_x\text{Ga}_{(1-x)}\text{N}$ films with two different high Al-contents ($x=0.43$ and 0.52) have been investigated by atomic force microscopy (AFM). The annealing treatments were performed in a nitrogen (N_2) gas ambient as short-time (4 min) and long-time (30 min). Firstly, the films were annealed as short-time in the range of $800\text{--}950\text{ }^\circ\text{C}$ in steps of $50\text{--}100\text{ }^\circ\text{C}$. The surface root-mean-square (rms) roughness of the films reduced with increasing temperature at short-time annealing (up to $900\text{ }^\circ\text{C}$), while their surface morphologies were not changed. At the same time, the degradation appeared on the surface of the film with lower Al-content after $950\text{ }^\circ\text{C}$. Secondly, the $\text{Al}_{0.43}\text{Ga}_{0.57}\text{N}$ film was annealed as long-time in the range of $1000\text{--}1200\text{ }^\circ\text{C}$ in steps of $50\text{ }^\circ\text{C}$. The surface morphology and rms roughness of the film with increasing temperature up to $1150\text{ }^\circ\text{C}$ did not significantly change. Above those temperatures, the surface morphology changed from step-flow to grain-like and the rms roughness significantly increased.

© 2009 Elsevier Ltd. All rights reserved.

1. Introduction

Wide band gap nitride semiconductors are most promising materials for electronic and optoelectronic devices due to superior material properties [1,2,3,4,5]. These materials are also remarkably tolerant of aggressive environments because of their thermal stability and radiation hardness [5]. It is rather well known that nitride materials are generally grown on sapphire substrates due to its low cost, thermal stability, and mature growth technology [6,7]. Unfortunately, different lattice parameters and thermal expansion coefficients of the nitride and sapphire materials cause large stresses in the grown epitaxial films. In this case, nitride films have poor

crystalline quality because of the introduction of cracks and defects into material as stress relieving mechanisms [8]. The preparation of good-quality nitride epitaxial films is quite important for high-performance device fabrication. Thermal annealing has been a powerful technique for improving the structural quality of epitaxial films in the growth of lattice mismatch systems [9,10,11,12,13,14]. Thermal annealing is also an important processing step in the fabrication of nitride based devices [8]. It has been reported that the annealing in a N_2 gas ambient between 900 and $1100\text{ }^\circ\text{C}$ considerably improved morphological and optical properties of GaN layers [13,14,15]. However, effects of the annealing on AlGaIn materials have not been completely clarified as of yet.

In the present work, we studied the effects of short- and long-time annealing on the morphological properties of $\text{Al}_x\text{Ga}_{(1-x)}\text{N}$ films with two different Al-contents ($x=0.43$ and 0.52) grown on sapphire substrates by metal-organic chemical vapor deposition (MOCVD). We

* Corresponding author. Tel.: +90 312 2126030;
fax: +90 312 2122279.

E-mail address: suleymancorekci@gazi.edu.tr (S. Çörekçi).

found that the Al-contents in AlGa_N films and annealing temperatures have significant influences on the morphological changes depending on annealing.

2. Experiments

About 400 nm-thick Al_xGa_(1-x)N films were grown on c-face sapphire substrates by MOCVD. Hydrogen (H₂) was used as the carrier gas and trimethylgallium (TMGa), trimethylaluminum (TMAI), and ammonia (NH₃) were used as the Ga, Al, and N sources, respectively. The films with two different high Al-contents ($x=0.43$ and 0.52) were labeled as samples A and B. A sequence of annealing treatments was performed in a N₂ gas ambient as short-time (4 min) and long-time (30 min). First of all, samples A and B were annealed at short-time (4 min) from 800 up to 950 °C in steps of 50–100 °C and then sample A with lower Al-content was annealed at long-time (30 min) from 1000 up to 1200 °C in steps of 50 °C. After annealing treatments, AFM measurements with two different scan areas ($5 \times 5 \mu\text{m}^2$ and $2 \times 2 \mu\text{m}^2$) were used to characterize the samples. AFM images of the samples were recorded using the needle mode operation on an Omicron VT STM/AFM. For the subsequent AFM measurements, each sample was cleaned by solvent rinsing: acetone (5 min), ethanol (5 min), and de-ionized H₂O, respectively. The measurements were carried out at room-temperature (RT) and atmosphere pressure. The rms

values from the surface topography were processed with Scala Pro software.

3. Results and discussion

Surface morphology of the AlGa_N films has a significant effect on the formation of contacts in devices. On the other hand, the effects of thermal annealing on the films are more evident near the surface [16]. Thus, AFM is a useful technique to characterize morphological properties of as-grown and annealed samples in this study. Fig. 1 shows the AFM images with $5 \times 5 \mu\text{m}^2$ and $2 \times 2 \mu\text{m}^2$ scan area of as-grown samples A and B and AFM line profiles on the images with $2 \times 2 \mu\text{m}^2$ scan area. There appear relatively parallel step-terraces and dark spots on the surfaces of both samples. The lateral sizes of the terraces that were obtained from AFM line profiles of samples A and B are approximately 85 and 79 nm. The dark spots on the surfaces travel deep into the AlGa_N epitaxial films and their diameters are in the range of 30–60 nm. The dark spot density of samples is approximately estimated as 10^7cm^{-2} from the ratio of the number of total dark spots to the scanned area. Step-terraces on the surface show that the AlGa_N epilayers are grown as step-flow. Step-flow growth mode is beneficial for device performance, because it creates a smoother surface [17,18]. However, the dark spots on the AlGa_N surface are known to have surface traps and they lead to current collapse and power

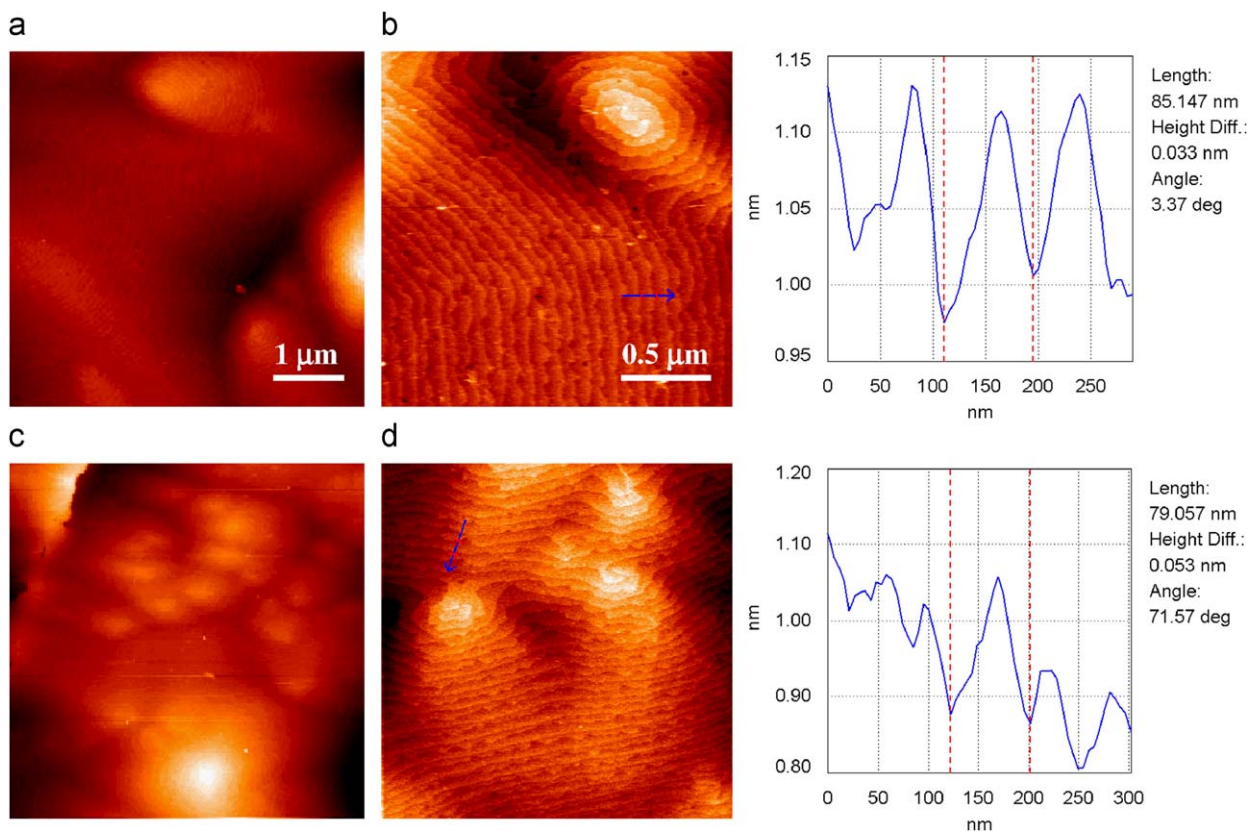


Fig. 1. AFM images with (a), (c) $5 \times 5 \mu\text{m}^2$ and (b), (d) $2 \times 2 \mu\text{m}^2$ scan area of as-grown samples A and B.

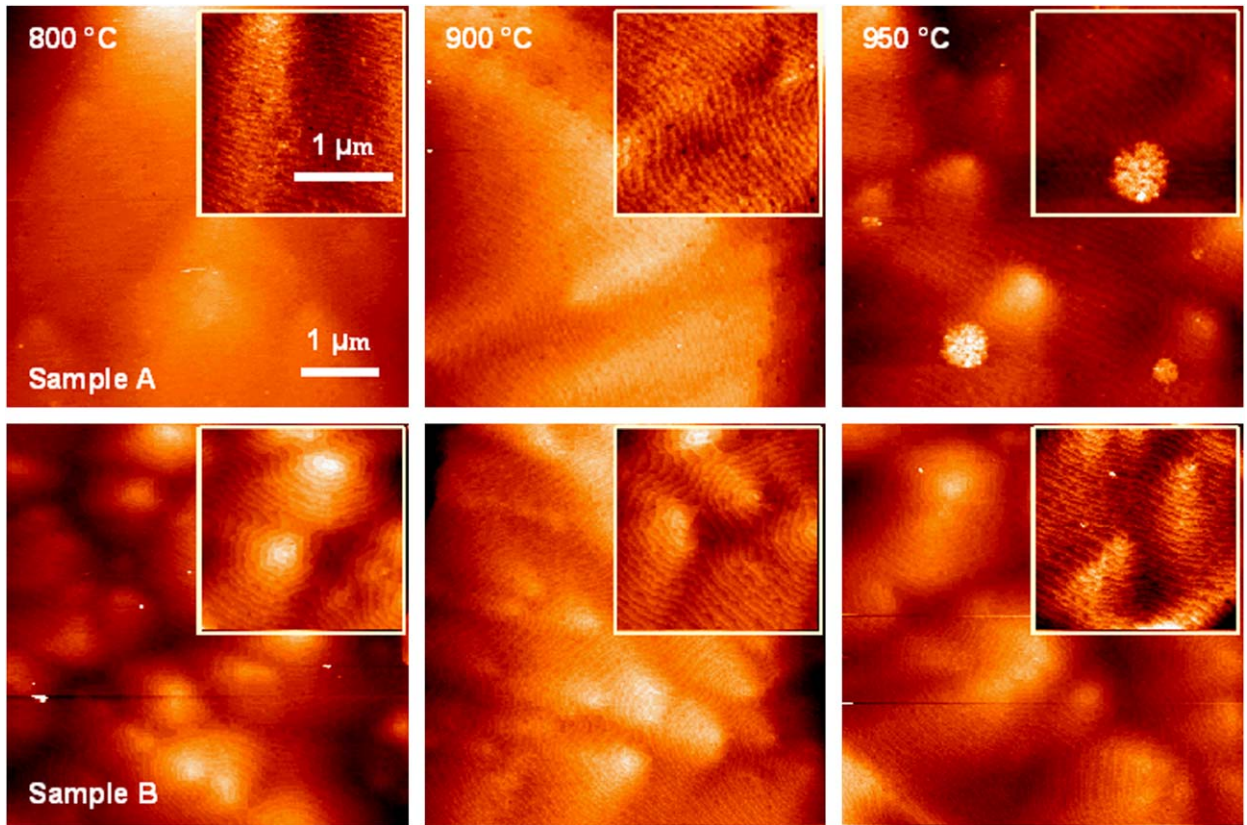


Fig. 2. AFM images with $5 \times 5 \mu\text{m}^2$ scan area of short-time annealed samples A and B. Inset shows the image with a $2 \times 2 \mu\text{m}^2$ scan area.

slump [19,20]. The surface rms roughnesses of samples A and B are obtained as 0.79 and 1.66 nm. A $2 \times 2 \mu\text{m}^2$ scan area is often relatively flat and is not an accurate representation of the surface, while the $5 \times 5 \mu\text{m}^2$ scan area is a much better representation of the surface. Thus, we used the rms values that were obtained with scan area of $5 \times 5 \mu\text{m}^2$ for quantifying the surface roughness. At the same time, the lateral sizes of the terraces on the surface are quite important to evaluate surface roughness. Due to the appearance of the laterally larger terraces on the surface, this suggests lower roughness on the surface [21,22]. As seen in Fig. 1, the lateral terrace sizes that were determined from line profiles are harmonious with the surface rms roughnesses of samples.

Fig. 2 shows AFM images with 5×5 and $2 \times 2 \mu\text{m}^2$ scan area of short-time annealed samples A and B from 800 until 950 °C. Below 950 °C, no morphological change on both samples has been observed. This result is in agreement with other experimental studies [23,24]. However, there appears a hillock-like structure with approximately 0.5–2.0 nm in height and on the order of 350–1000 nm in diameter on the surface of sample A after 950 °C annealing. On the contrary in sample A, there is no change on the step-flow morphology of sample B. The degradation on the surface of sample A can be related to the thermal stability of sample A due to its low Al content. This result shows that the Al-contents in films have a significant influence on morphological change. Fig. 3

shows the variation of the surface rms roughness as a function of annealing temperature for samples. The rms roughness of sample A slightly reduced until surface degradation (from 0.79 to 0.72 nm) and then the rms roughness (0.94 nm) increased as a result of increasing annealing temperature. However, the surface rms roughness of sample B was reduced from 1.66 to 0.74 nm. The smoother surface is related to the reducing defect density and removing impurities on the surface of samples after short-time annealing [2,14,15].

Fig. 4 shows AFM images with 5×5 and $2 \times 2 \mu\text{m}^2$ scan area of long-time annealed sample A from 1000 to 1200 °C. As seen in Fig. 4, there is no change in the step-flow surface morphology of the sample up to 1150 °C annealing except for hillock-like degradation. However, there appear grains with approximately 50–150 nm in size on the sample after 1150 °C annealing and its surface morphology is changed from the step-flow to grain-like. Kuball et al. [25] reported that AlGaIn material degraded for annealing temperatures higher than 1150 °C using the Raman scattering. Note that a large amount of strain builds in the AlGaIn film prior to its degradation at 1150 °C. Stress changes during annealing in a N_2 gas ambient that are attributed to morphological changes in the sample [8,25]. Thus, the change on the surface morphology of sample A is probably related to the relaxation of the residual stress in the AlGaIn layer. On the other hand, the grain sizes on the surface are reduced

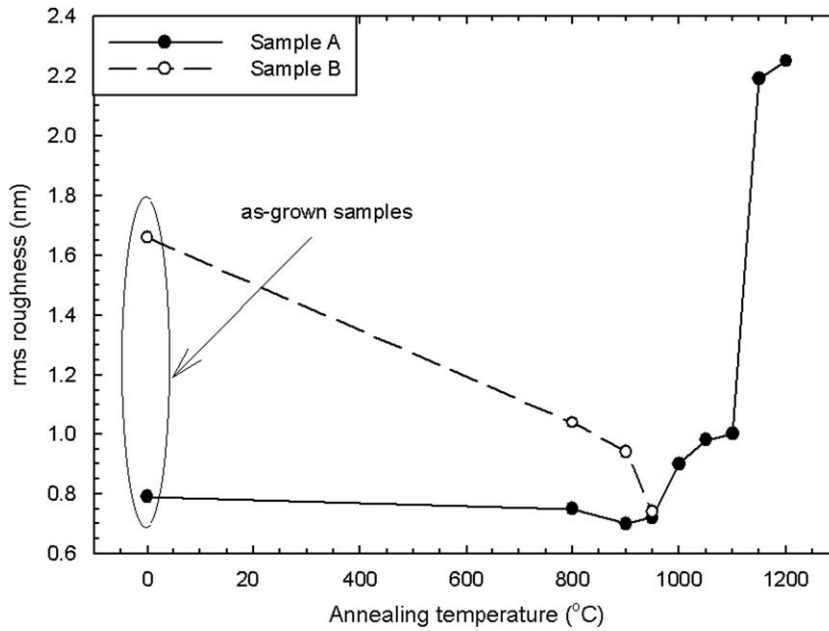


Fig. 3. The variation of the surface rms values of samples A and B that were obtained from the AFM measurements with $5 \times 5 \mu\text{m}^2$ scan areas as a function of annealing temperature.

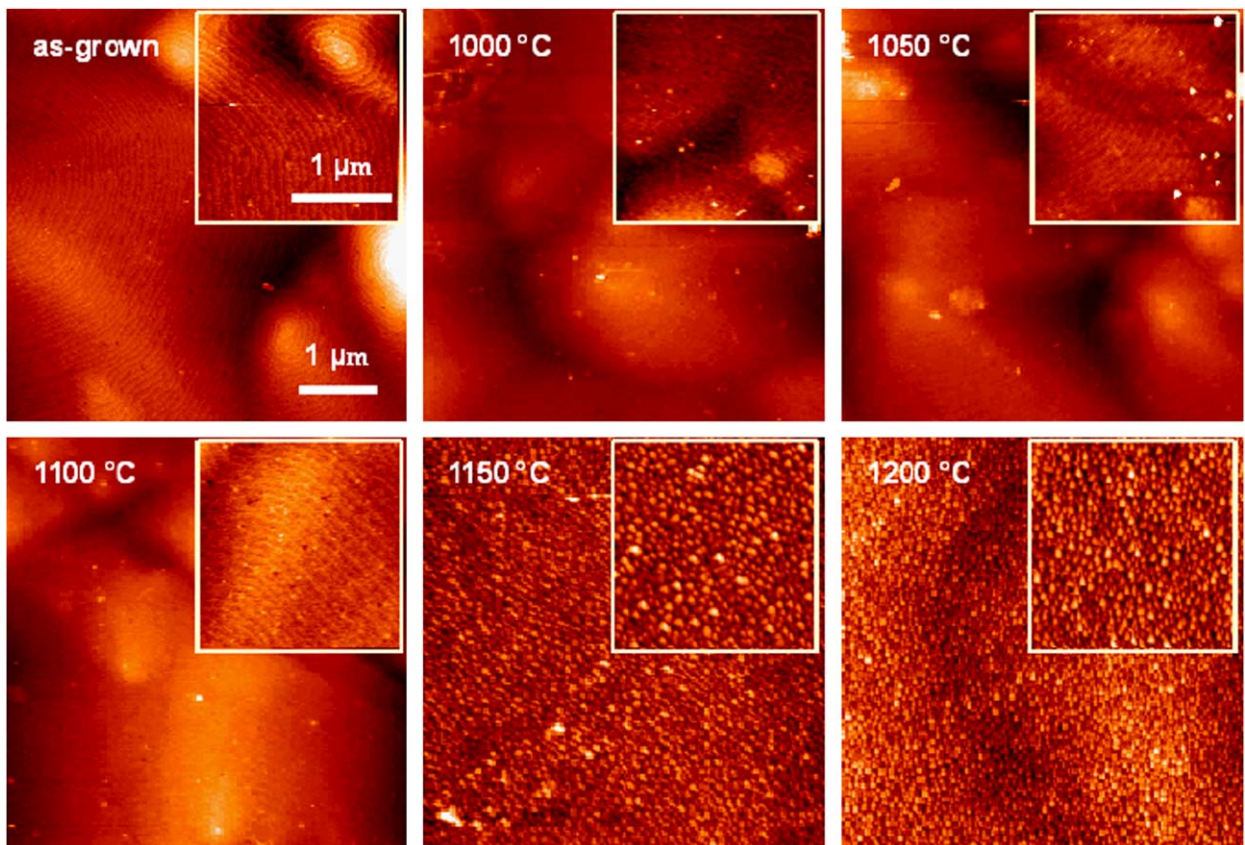


Fig. 4. AFM images with $5 \times 5 \mu\text{m}^2$ scan area of long-time annealed sample A. Inset shows the image with a $2 \times 2 \mu\text{m}^2$ scan area.

from 50–150 to 40–120 nm after 1200 °C annealing. Tao et al. [26] investigated the effects of annealing on mosaic structure of GaN films and found that lateral coherence length has an important influence on the (0002) full-width at half-maximum (FWHM). In their study, the increase of (0002) FWHM together with the decrease of lateral coherence lengths is attributed to the increase of edge-type dislocation density during annealing. Within this framework, the reduction in the grain sizes on the surface of sample A after annealing from 1150 to 1200 °C shows that sample A has poorer crystalline quality. These results clearly indicate that the annealing temperature for AlGa_N films is rather critical from the viewpoint of structural quality. In addition, as shown in Fig. 3, the surface rms roughness of sample A slightly enhanced with increase in temperature (up to 1150 °C). Moreover, the rms roughness significantly increased along with the change from step-flow to grain-like of the surface morphology after 1150 °C annealing. XPS results show that the stoichiometry of the surface is changed with increased annealing temperature. Accordingly, Ga and Al move deeper into the surface and N goes to the top surface as the temperature is increased [2]. The increase in rms roughness and change in morphology of sample A are probably with this effect on the surface of AlGa_N film. AFM measurements obtained from both short- and long-time annealing treatments clearly show that the best annealing temperature for the Al_{0.43}Ga_{0.57}N film with relatively low content (sample A) is around 900 °C, which is an agreement with another report [4].

Recently, Liu et al. [24] investigated the effect of thermal annealing on the morphological and structural properties of AlN thin films. They found that the annealing improves the crystalline quality of the AlN films up to 1000 °C. After 1000 °C annealing, the poorer crystalline quality of the films was attributed to the decomposition and degradation of AlN films. In their study, the surface rms roughness of the AlN films has no significant change up to 1000 °C. However, the rms roughness of the films increased significantly after annealing at higher temperature. Therefore, it is concluded that AlN films keep stable below 1000 °C. The experimental results regarding annealed AlN and AlGa_N thin films seem to be occurring in harmony. Finally, both previous reports and our study clearly show that the high annealing temperatures (above 1000 °C) are not good for AlGa_N films with high Al-contents due to the thermal damage on the surfaces.

4. Conclusion

Effects of thermal annealing on the morphology of the Al_{0.43}Ga_{0.57}N and Al_{0.52}Ga_{0.48}N films with two different Al-contents have been investigated by AFM. The annealing treatments were performed in N₂ gas ambient as short- and long-time. It is found that the Al-contents in films and annealing temperatures have significant influences on the morphological changes. AFM measurements show that

the surface rms roughness of both films with increase in temperature at short-time annealing up to 900 °C are reduced but their surface morphologies are not changed. However, degradation occurred on the surface of the film with lower Al-content after 950 °C. Moreover, surface morphology of the same film changed from step-flow to grain-like and the rms roughness significantly increased after 1150 °C long-time annealing.

Acknowledgment

This work was supported by the Turkish State Planning Organization (Project no. 2001K120590) and by TUBITAK under Project Nos. 104E090, 105E066, and 105A005. One of the authors (E. O.) also acknowledges partial support from the Turkish Academy of Sciences.

References

- [1] Razeghi M, Rogalski A. *J Appl Phys* 1996;79:7433.
- [2] Boudjelida B, Simmonds MC, Gee I, Clark SA. *Appl Surf Sci* 2006;252:5189.
- [3] Xing H, Keller S, Wu Y-F, McCarthy L, Smorchkova IP, Buttari D, et al. *J Phys: Condens Matter* 2001;13:7139.
- [4] Obata T, Hirayama H, Aoyagi Y, Ishibashi K. *Phys Stat Sol A* 2004;201:2803.
- [5] Ko TK, Chang SJ, Su YK, Lee ML, Chang CS, Lin YC, et al. *J Cryst Growth* 2005;283:68.
- [6] Yu H, Caliskan D, Ozbay E. *J Appl Phys* 2006;100:033501.
- [7] Lester SD, Ponce FA, Craford MG, Steigerwald DA. *Appl Phys Lett* 1995;66:31249.
- [8] Rajasingam S, Sarua A, Kuball M, Cherodian A, Miles MJ, Younes CM, et al. *J Appl Phys* 2003;94:6366.
- [9] Chand N, People R, Baiocchi FA, Wetck KW, Cho AY. *Appl Phys Lett* 1986;49:815.
- [10] Matyi RY, Lee JW, Schaake HF. *J Electron Mater* 1988;17:87.
- [11] Yamaguchi M, Tachikawa M, Itoh Y, Sugo M, Kondo S. *J Appl Phys* 1990;68:4518.
- [12] Kumar MS, Sonia G, Ramakrishnan V, Dhanasekaran R, Kumar J. *Physica B* 2002;324:223.
- [13] Siegle H, Kaczmarczyk G, Filippidis L, Litvinchuk AP, Hoffmann A, Thomsen C. *Phys Rev B* 1997;55:7000.
- [14] Hong J, Lee JW, MacKenzie JD, Donovan SM, Abernathy CR, Pearton SJ, et al. *Semicond Sci Technol* 1997;12:1310.
- [15] Zolper JC, Crawford MH, Howard AJ, Ramer J, Hersee SD. *Appl Phys Lett* 1996;68:200.
- [16] Oh E, Kim B, Park H, Park Y. *Appl Phys Lett* 1998;73:1883.
- [17] Stephenson GB, Eastman JA, Thompson C, Auciello O, Thompson LJ, Munkholm A, et al. *Appl Phys Lett* 1999;74:3326.
- [18] Bai J, Dudley M, Sun WH, Wang HM, Asif Khan A. *Appl Phys Lett* 2006;88:051903.
- [19] Veturly R, Zhang NQ, Keller S, Mishra UK. *IEEE Trans Electron Dev* 2001;48:560.
- [20] Binari SC, Ikossi K, Roussos JA, Kruppa W, Park D, Dietrich HB, et al. *IEEE Trans Electron Dev* 2001;48:465.
- [21] Torabi A, Ericson P, Yarranton EJ, Hooke WE. *J Vac Sci Technol B* 2002;20:1234–7.
- [22] Çörekçi S, Öztürk MK, Akaoglu B, Çakmak M, Özçelik S, Özbay E. *J Appl Phys* 2007;101:123502.
- [23] Kuball M, Demangeot F, Frandon J, Renucci MA, Massies J, Grandjean N, et al. *Appl Phys Lett* 1998;73:960.
- [24] Liu B, Gao J, Wu KM, Liu C. *Solid State Commun* 2009;149:715.
- [25] Kuball M, Demangeot F, Frandon J, Renucci MA, Sands H, Btchelder DN, et al. *Appl Phys Lett* 1999;74:549.
- [26] Tao CZ, Ke X, Ping GL, Jian YZ, Bo PY, Yong SY, et al. *Chin Phys Lett* 2006;23:1257.